19th International Congress on Modelling and Simulation, Perth, Australia, 12–16 December 2011
http://mssanz.org.au/modsim2011

Cross-border pollution by SO_x in East Asia based on GCM output considering future global warming

Y. Suzuki [a], S. Watanabe [b] and M. Hasebe [c]

[a] *Dept. of Civil and Environmental Engineering, Faculty of Engineering and Design, Hosei University, Japan*
[b] *Utsunomiya municipal office, Japan*
[c] *Graduate School of Engineering, Utsunomiya University, Japan*
Email: y-suzuki@hosei.ac.jp

Abstract: After the 1990s, sulphur oxide (SO_x) emissions from human activities, one of the main causes of acid rain, have been consistently increasing in the Asian region. Especially, in mainland China showing rapid industrialization, a large amount of SO_x (mainly as SO_2) is discharged every year, which can be transported to Japan by atmospheric advection, which can become an issue of serious public concern. If the current tendency of global warming continues and advances, variations of the atmospheric field in the near future would affect cross-border pollution by acid materials, and therefore, countermeasures should be devised based on environmental impact assessment considering climate change in the future.

In the current study, with the aim of achieving local assessment in East Asia under the influence of future climate change, advection and dispersion simulations about SO_2 discharged from mainland China were conducted using the numerical model HYSPLIT4 (Hybrid Single-Particle Lagrangian Integrated Trajectory Model Version 4). As atmospheric datasets for the model input, the current study employed GCM (Global Climate Model) output, provided by the Innovative Program of Climate Change Projection for the 21st Century (KAKUSHIN Program) in Japan. The datasets were computed with a boundary condition of sea surface temperature representing the effect of future global warming (A1B scenario of IPCC). Wintertime datasets for 25 years of 1980 to 2004 were used for the present condition and those of 2075 to 2099 were for the future condition.

Firstly, to see how the atmospheric field (wind velocity and water vapour) in East Asia tends to vary with climate change in the future, a pattern classification technique of Self-Organizing Maps (SOMs) was applied to the atmospheric datasets with 6-hour intervals. SOMs, one of Artificial Neural Networks (ANNs) with unsupervised learning, can provide a two-dimensional map classifying a complicated pattern of nonlinear and multi-dimensional data. Consequently, the atmospheric field on the present and future conditions were classified into mainly 7 patterns, and the occurrence frequency of each atmospheric pattern was computed respectively for the present and future conditions. The minimum frequency among the 7 patterns is around 2 % and the maximum is around 20 %, and two of them show a significant increase of the frequency on the future condition, while two patterns show a significant decrease and the remaining three show a slight change only.

Secondly, advection and dispersion simulations by HYSPLIT4 were conducted using datasets of the atmospheric field representing each of the 7 patterns, and the air concentration and deposition amount of SO_x was computed to see how and where the influence of SO_2 discharged from mainland China could become intensified. In the model, puffs or particles were traced using the Lagrangian approach, and three processes of advection, dispersion and deposition are computed in turn. The horizontal resolution was set to 0.15 by 0.15 degrees, and vertical layer from the ground to the altitude of 3000 m was divided into 8 layers. The amount of SO_2 discharged from China was determined based on data for 2005 reported in China, and 9 points located in the eastern part of China with a relatively large SO_2 emission were chosen as emission sources.

Simulation results show, in the atmospheric pattern with a frequency increase on the future condition, SO_x tends to be advected in the northern or northeastern direction, and the total amount of its deposition tends to be larger in the northern part of China and Japan or around the Korean Peninsula. In this pattern, the amount of SO_x deposition as a whole including that in other Asian regions shows a tendency to be larger than other atmospheric patterns, which can be attributed to its higher specific humidity in the atmosphere, producing greater wet deposition. This result is consistent with the expectation that the amount of atmospheric water vapour will increase in the future due to the progress of global warming.

Keywords: *cross-border pollution, sulphur dioxide, global warming, advection and dispersion model*

1. INTRODUCTION

In some regions of Japan, rainfall with a high acidity of pH 4 is observed, and there is rising concern about its influence on the water and soil environment, and ecosystem functions. After the 1990s, sulphur oxide (SOx) emissions from human activities, one of the main causes of acid rain, have been consistently increasing in the Asian region. Especially, in mainland China showing rapid industrialization, a large amount of SO_x (mainly as SO_2) is discharged every year, which can be transported to Japan by atmospheric advection. Taking into consideration that environmental measures against air pollution have been insufficient in China, the influence of acid rain and acid deposition could be revealed in Japan, which can become an issue of serious public concern.

On the other hand, if the current tendency of global warming continues and advances, variations of the atmospheric field in the near future would deeply affect cross-border pollution by SO_x, and therefore, countermeasures should be devised based on environmental impact assessment considering climate change in the future. In the current study, with the aim of achieving local assessment in East Asia under the influence of future climate change, advection and dispersion simulations about SO_2 discharged from mainland China were conducted using the numerical model HYSPLIT4 (Hybrid Single-Particle Lagrangian Integrated Trajectory Model Version 4).

As atmospheric datasets for the model input, the current study employed GCM (Global Climate Model) output with a horizontal resolution of 1.25 by 1.25 degrees, provided by the Innovative Program of Climate Change Projection for the 21st Century (KAKUSHIN Program) in Japan (Kitoh *et al.*, 2009). The datasets were computed with a boundary condition of sea surface temperature representing the effect of future global warming (A1B scenario of IPCC). Specifications of the datasets are shown in Table 1. Wintertime datasets at 6-hour intervals for 25 years from 1980 to 2004 were used for a present condition and that from 2075 to 2099 for a future condition.

2. PATTERN CLASSIFICATION USING SELF-ORGANIZING MAPS (SOMS)

Firstly, to see how the atmospheric field (wind velocity and water vapour) in East Asia tends to vary with climate change in the future, a pattern classification technique of Self-Organizing Maps (SOMs) was applied to the atmospheric datasets. SOMs, one of Artificial Neural Networks (ANNs) with unsupervised learning, can provide a two-dimensional map classifying a complicated pattern of nonlinear and multi-dimensional data (Kohonen, 1995).

In the current study, the East Asian region around the Sea of Japan was divided into 16 blocks, as

Table 1. Specifications of the GCM atmospheric datasets, provided by the KAKUSHIN Program.

Model name	MRI-AGCM3.1S
Horizontal resolution of the model	20 by 20 km
Horizontal resolution of output datasets	1.25 by 1.25 degrees
Time interval	6-hour intervals
Number of the vertical layers in output datasets	9 layers from 925 to 150 hPa
Period of time defined as a present condition	25 years from Jan. 1980 to Dec. 2004
Period of time defined as a future condition	25 years from Jan. 2075 to Dec. 2099
Output elements with three dimensions	wind velocity, temperature, specific humidity, etc.

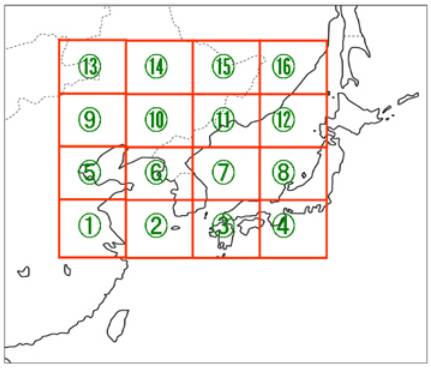

Figure 1. Study region around the Sea of Japan in the East Asia, and 16 divided blocks in which areal average datasets were created for SOMs.

Table 2. Initial conditions used for the training of SOMs in the first classification for downsampling and the second applied to representative vectors.

	First	Second
Map size	10 by 10	20 by 10
Dimensions of an input vector	48 (=16 x 3)	←
Number of input vectors	8640 for each condition	200 in total (=100+100)
Number of training iteration	a half million	a million
Initial learning rate	0.2	←
Initial neighborhood radius	15	25

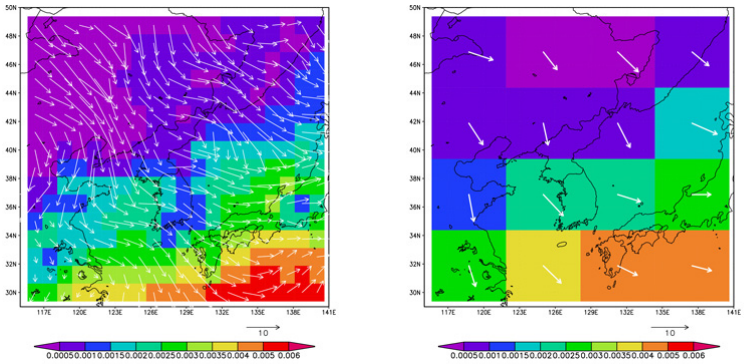

(a) original datasets (b) created datasets

Figure 2. An example of the atmospheric datasets, (a) original one with a horizontal resolution of 1.25 by 1.25 degrees, and (b) created one averaged in respective 16 blocks.

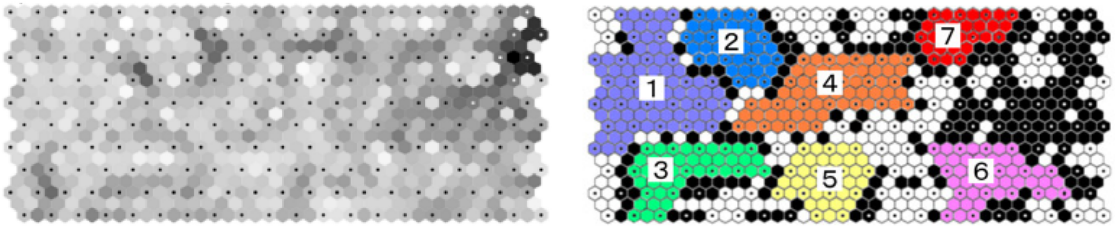

(a) U-matrix representation (b) classification into 7 clusters

Figure 3. Classification result for 200 representative vectors visualized in a two-dimensional map with 20 by 10 nodes using the U-matrix representation, and its corresponding map of classification into 7 clusters based on the distance and colour on the U-matrix representation.

shown in Figure 1, and areal average data in each block were created for meridional wind velocity, zonal wind velocity and specific humidity at 6-hour intervals at an altitude of 925 (hPa), approximately 700 (m) above sea level. Figure 2 shows an example of the original and created datasets, in which the arrows show wind vector and the colour contours show specific humidity. Such 48-dimensional vector datasets (16 blocks and 3 types) were normalized and employed as the input for the pattern classification by SOMs.

As shown in Table 2, the number of input vectors at 6-hour intervals for 25 years is 8640 respectively for the present and future conditions, and it could be a problem to apply SOMs to such a large dataset. Therefore, the current study introduced a two-step approach described below using SOMs twice to obtain an appropriate result of pattern classification.

(1) first classification conducted for downsampling to extract 100 winning vectors under each of the two conditions (present and future)

(2) second classification applied to the combined datasets of 200 (=100+100) obtained above as representative vectors

The first step is based on the fact that winning vectors obtained by SOMs generally represent characteristics of input vectors. After the two steps, the classification result for representative vectors was visualized in a two-dimensional map using the U-matrix (unified distance matrix) representation, in which the similarity of two vectors allocated to adjacent nodes is represented by both the distance on the map and grey scale colour. Darker colours show lower similarity and can also be a boundary of classification. The current study set a threshold value in the colour scale to 70 % of the darkest to clarify the boundaries, and classified the whole area on the map into some regions (clusters).

As shown in Figure 3, representative vectors were consequently classified into mainly 7 clusters, meaning that the atmospheric field on the present and future conditions can be classified into mainly 7 patterns. Based on this result, the current study computed the proportion of input vectors classified into each cluster to the total of 8640, that is the occurrence frequency of each atmospheric pattern, respectively for the present and future conditions, as well as examined characteristics of the atmospheric pattern in each cluster.

Table 3. Proportion of input vectors classified into each cluster to the total of 8640, that is the occurrence frequency of each atmospheric pattern, respectively for the present and future conditions.

Cluster No.	1	2	3	4	5	6	7	Total
Present condition	21.5%	10.0%	6.81%	14.9%	6.41%	6.00%	2.32%	67.9%
Future condition	11.9%	4.33%	6.97%	13.2%	4.64%	10.3%	5.47%	56.8%
Grouping	A		C			B		

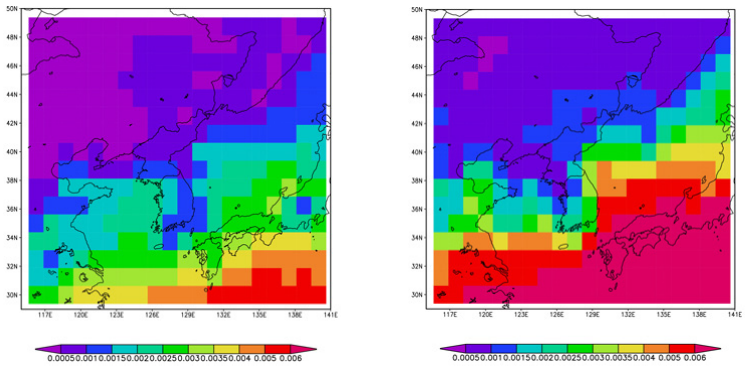

(a) No.1 (b) No.7

Figure 4. An example of the field of specific humidity in the cluster No.1 and No.7.

Table 3 shows the result that the minimum occurrence frequency is around 2 % and the maximum around 20 %, and two of them (cluster No.1 and No.2) show a significant decrease of the frequency on the future condition, while another two (cluster No.6 and No.7) show a significant increase and the remaining three (cluster No.3, No.4 and No.5) show a slight change only. The total percentage on the future condition is significantly smaller than that on the present condition, indicating that exceptional (abnormal) patterns with a low occurrence frequency can increase in the future. Sampling examination into characteristics of the atmospheric patterns in each cluster confirmed the validity of the classification.

One of the differences between the clusters No.1, No.2 and No.6, No.7 lies in the average value of specific humidity, that of the latter frequently shows a higher value, meaning that specific humidity tends to be higher on the future condition. Figure 4 shows an example of the field of specific humidity in the cluster No.1 and No.7. A group of atmospheric fields classified into the cluster No.1, No.2 is denoted as Group A, No.6, No.7 as Group B, and No.3, No.4, No.5 as Group C as shown in Table 3.

The current study extracted some 5-day periods including a relatively large number of atmospheric fields classified into Group A, B and C respectively, and conducted advection and dispersion simulations about SO_2 discharged from mainland China in the winter season using such atmospheric fields and the numerical model HYSPLIT4, as mentioned in the next section. A group of periods including a large number of atmospheric fields classified into Group A is denoted as Periods A, Group B as Periods B, and Group C as Periods C.

3. ADVECTION AND DISPERSION SIMULATIONS USING HYSPLIT4

3.1. Model and data descriptions

HYSPLIT4 (Hybrid Single-Particle Lagrangian Integrated Trajectory Version 4) is an advection and dispersion model developed by Draxler et al. (Draxler and Taylor, 1982; Draxler, 1992; Draxler and Hess, 2004). This model assumes materials can be represented by particles or puffs (or both) and calculates their advection, dispersion and deposition processes based on the Lagrangian approach. Air concentration calculations associate the mass of the pollutant species with the release of either puffs, particles, or a combination of both. The dispersion rate is calculated from the vertical diffusivity profile, wind shear, and horizontal deformation of the wind field. Air concentrations are calculated at a specific grid point for puffs and as cell-average concentrations for particles. The current study conducted simulations with a chemical conversion module, which includes gas- and aqueous-phase oxidation of SO_2 and dry and wet removal of SO_2 and SO_x particles.

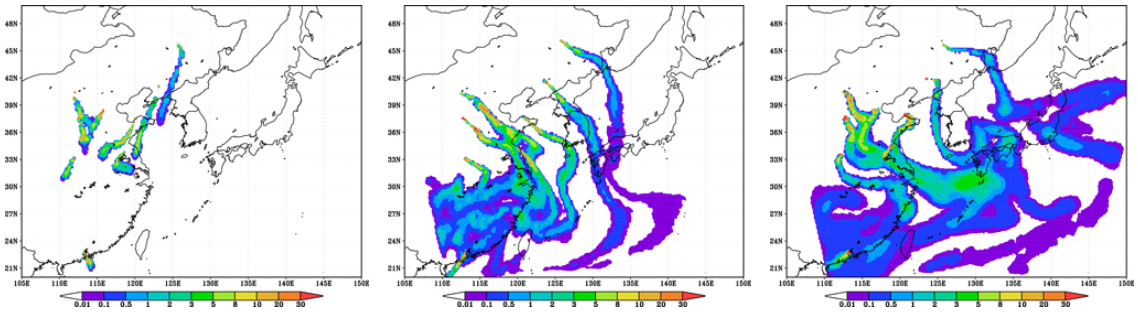

(a) 1 day after (b) 3 days after (c) 5 days after

Figure 5. An example of air concentration (ppb) of SO_x in the layer of 0-250 m in the Periods A, computed with an atmospheric field from 1 Feb. at 12:00 to 6 Feb. at 12:00 in 1983.

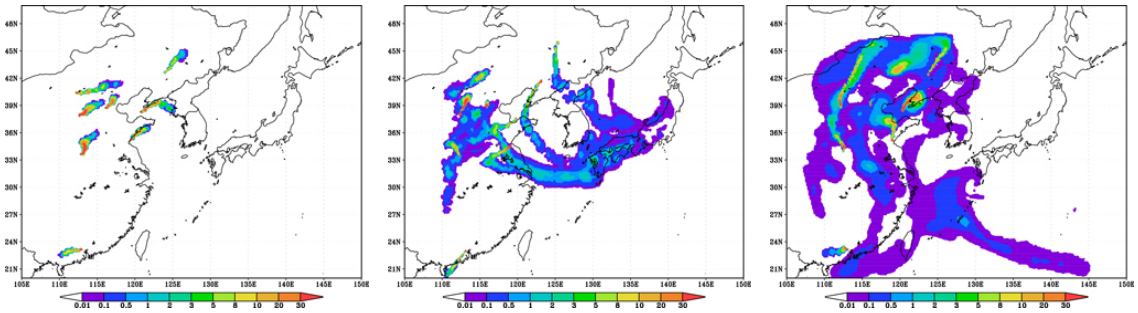

(a) 1 day after (b) 3 days after (c) 5 days after

Figure 6. An example of air concentration (ppb) of SO_x in the layer of 0-250 m in the Periods B, computed with an atmospheric field from 20 Feb. at 0:00 to 25 Feb. at 0:00 in 2098.

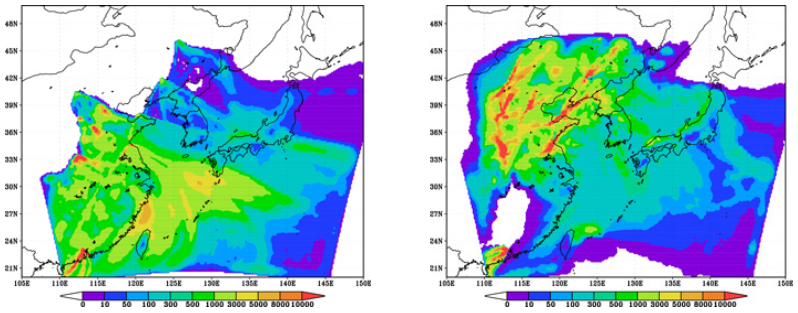

(a) Periods A (b) Periods B

Figure 7. An example of the total deposition amount ($\mu g/m^2$) of SO_x in the Periods A and B, computed in the same case as Figure 5 (Periods A) and Figure 6 (Periods B).

In the current study, the calculation domain was set to be the region with 30 degrees of latitude and 45 degrees of longitude, with the centre of the domain located at latitude 35.0 degrees north and longitude 127.50 degrees east. The horizontal resolution of the model grid was set to be 0.15 by 0.15 degrees, and the vertical grid was divided into 8 layers of the ground level, 0-250 m, 250-500 m, 500-750 m, 750-1000 m, 1000-1500 m, 1500-2000 m and 2000-3000 m. The release rate of SO_2 discharged from mainland China in the winter season were determined based on the 2005 dataset in the official report published in mainland China in 2006. The current study chose 9 points with a large amount of SO_2 emission in the eastern part of China as its emission sources. A period of time for each simulation is 120 hours (5 days), during which the release of SO_2 is assumed to continue with a constant release rate.

In order to conduct a precise analysis about the advection and dispersion of SO_2, the current study created datasets of atmospheric fields with a higher resolution by downscaling the GCM datasets used for pattern classification in the previous section. One of physical downscaling techniques was employed in the current study, based on numerical simulations using the mesoscale meteorological model MM5, a commonly-used model with a lot of achievements in various fields. Detailed descriptions of the model, found in many literatures (e.g. Suzuki et al., 2007), are omitted in this paper. In the current study, the horizontal resolution of the model grid was set to be 20 by 20 km, that is output datasets of atmospheric fields have a higher resolution

Table 4. Estimated average air concentration (ppb) of SO_x in the layer of 0-250 m on the present and future condition, based on simulation results and the values of proportion in Table 3.

Area	North Korea	South Korea	Taiwan	Okinawa Region	Chugoku Region	Kanto Region	Tohoku Region
Present condition	0.30	0.18	0.057	0.035	0.12	0.11	0.019
Future condition	0.59	0.49	0.022	0.060	0.15	0.12	0.051
Ratio	1.97	2.72	0.39	1.71	1.25	1.09	2.68

Table 5. Estimated total deposition amount ($\mu g/m^2$) of SO_x on the present and future condition, based on simulation results and the values of proportion in Table 3.

Area	North Korea	South Korea	Taiwan	Okinawa Region	Chugoku Region	Kanto Region	Tohoku Region
Present condition	358	174	319	232	128	121	14
Future condition	718	1280	77	135	388	290	60
Ratio	2.01	7.36	0.24	0.58	3.03	2.40	4.29

than that of original 1.25 by 1.25 degrees. To reduce errors in downscaling, the current study optimized nudging coefficients used for data assimilation on a trial-and-error basis, and confirmed the validity of the downscaling technique by comparison between original and output datasets.

3.2. Advection and dispersion of SO_2 in the winter season

Using the output datasets of MM5, advection and dispersion simulations about SO_2 discharged from mainland China in the winter season were conducted for each of the three groups of period, Periods A, B and C. Figure 5 shows an example of air concentration of SO_x in the Periods A, 1 day, 3 days and 5 days after the initial time, computed with an atmospheric field from 20 Feb. at 0:00 to 25 Feb. at 0:00 in 2098, and Figure 6 shows that in the Periods B, computed with an atmospheric field from 20 Feb. at 0:00 to 25 Feb. at 0:00 in 2098. As shown in these figures, simulation results of Periods A tend to show an advection of SO_x in a southerly or southeasterly direction, while those of Periods B show an advection in a northerly or northeasterly direction.

On the other hand, Figure 7 shows an example of the total deposition amount of SO_x in the Periods A and B, computed in the same case as Figure 5 and 6. There is a tendency for a large amount of deposition in Periods A to be in the eastern part of China or the southern part of Japan including Okinawa islands, while that in Periods B to be in northern part of China including the neighbourhood of Beijing. Especially, the deposition amount in Periods B tends to have the largest area with a high value over 1000 ($\mu g/m^2$) in the three groups of period, which can be attributed to the tendency of Periods B to have relatively higher specific humidity. An increase in the amount of wet deposition would be caused by such high humidity in Periods B, which is consistent with the expectation that the amount of atmospheric water vapour will increase in the future due to the progress of global warming.

To do local impact assessments in East Asia, the current study computed an estimated value of the average air concentration of SO_x in the layer of 0-250 m and the total deposition amount of SO_x on the present and future condition, based on simulation results and the values of proportion in Table 3. The values in Table 3 representing the occurrence frequency of each cluster were used as a weight. As shown in Table 4 and 5, assessments were conducted in the three neighbouring countries of Japan, i.e. North Korea, South Korea and Taiwan, and in the four domestic regions, i.e. Okinawa, Chugoku, Kanto and Tohoku regions.

As for the air concentration shown in Table 4, North and South Korea show its increase on the future condition, especially the value of South Korea increases to nearly three times as large as the present condition, while Taiwan shows a significant decrease. In the domestic regions as well, the air concentration tends to increase on the future condition. The rate of increase in Tohoku region is remarkably large, although the value of concentration itself is still less than the environmental criteria of Japan.

On the other hand, the deposition amount in Table 5 shows a significant increase on the future condition in two countries except Taiwan and three regions except Okinawa. Especially, the amount of 1280 ($\mu g/m^2$) and its rate of increase of approximately 6 times in South Korea are remarkably large, which could lead to a great negative influence on soil and water environments. Among the domestic regions, Chugoku region has the largest amount of deposition on the future condition, which could cause a concern for an environmental negative impact, although Tohoku has the largest rate of increase.

4. SUMMARY

The current study conducted advection and dispersion simulations about SO_2 discharged from mainland China using the numerical model HYSPLIT4 (Hybrid Single-Particle Lagrangian Integrated Trajectory Model Version 4). As atmospheric datasets for the model input, the current study employed GCM (Global Climate Model) output provided by the Innovative Program of Climate Change Projection for the 21st Century (KAKUSHIN Program) in Japan.

To see how the atmospheric field (wind velocity and water vapour) in East Asia tends to vary with climate change in the future and to extract representative atmospheric fields for the simulation, a pattern classification technique of Self-Organizing Maps (SOMs) was applied to the atmospheric datasets with 6-hour intervals. The atmospheric field on the present and future conditions were classified into mainly 7 patterns, and the occurrence frequency was computed for each of them. Two patterns (Group A) show a significant increase of the frequency on the future condition, while two of them (Group B) show a significant decrease and the remaining three (Group C) show a slight change only.

Results of simulations conducted based on the pattern classification show different tendencies in the direction of advection and the deposition amount of SO_x among the three groups of period (Periods A, B and C). There is a tendency for a large amount of deposition in Periods A to be in the eastern part of China or the southern part of Japan including Okinawa islands, while that in Periods B to be in northern part of China including the neighbourhood of Beijing and have the largest area with a high value over 1000 ($\mu g/m^2$) in the three groups of period, which can be attributed to the tendency of Periods B to have relatively higher specific humidity.

In local impact assessments, the deposition amount shows a significant increase on the future condition in two countries except Taiwan and three regions except Okinawa. Especially, the amount of 1280 ($\mu g/m^2$) and its rate of increase of approximately 6 times in South Korea are remarkably large, which could lead to a great negative influence on soil and water environments. Among the domestic regions, Chugoku region has the largest amount of deposition on the future condition, which could cause a concern for an environmental negative impact in the future.

ACKNOWLEDGMENTS

This work was conducted under the framework of the "Projection of the change in future weather extremes using super-high-resolution atmospheric models" supported by the KAKUSHIN Program of the Ministry of Education, Culture, Sports, Science, and Technology (MEXT).

REFERENCES

Kitoh, A. T. Ose, K. Kurihara, S. Kusunoki, M. Sugi and KAKUSHIN Team-3 Modeling Group (2009), Projection of changes in future weather extremes using super-high-resolution global and regional atmospheric models in the KAKUSHIN Program: Results of preliminary experiments, *Hydrological Research Letters*, 3, 49-53. doi:10.3178/hrl.3.49

Kohonen, T. (1995), Self-Organizing Maps, *Springer Series in Information Sciences*, Vol.30.

Draxler, R. R., and Taylor, A. D. (1982), Horizontal dispersion parameters for long-range transport modeling, *J. Appl. Meteorol.*, 21, 367-372.

Draxler, R. R. (1992), Hybrid single-particle Lagrangian integrated trajectories (HY-SPLIT) Version3.0 User's guide and model description, NOAA Tech. Memo. ERL ARL-195.

Draxler, R. R. and Hess, G. D. (2004), Description of the HYSPLIT4 MODELING SYSTEM, NOAA Tech. Memo. ERL ARL-224.

Suzuki, Y., S. Miyata, E. Nakakita, and M. Hasebe (2007), Numerical approach on the mechanism of precipitation-topography relationship in mountainous complex terrain, Proc. of International Congress on Modelling and Simulation 2007 (MODSIM07), pp.2131-2137.